Sensor Applications

An Affordable Inkjet-Printed Foot Sole Sensor and Machine Learning for Telehealth Devices

Steven Gardner[1*], Adnan Porbanderwala[2], and Mohammad R. Haider[1*]
[1]School of Engineering, The University of Alabama at Birmingham, Birmingham, AL 35294, USA
[2]College of Engineering, Georgia Institute of Technology, Atlanta, GA 30332, USA
[*]Member, IEEE

Manuscript received xx xx, xxxx; revised xx xx, xxxx; accepted xx xx, xxxx. Date of publication xx xx, xxxx; date of current version xx xx, xxxx.

Abstract—Reduction of cardiovascular disease risk is highly correlated with regularity of exercise, which is not easily observed outside of medical settings, particularly for the elderly. Foot sole monitoring technology is now a saturated market due to its demand for applications in physical therapy, sports, hazardous work, etc. However, the best technology available comes with drawbacks like high prices, bulkiness, discomfort, and low power efficiencies. This work seeks to resolve many of these shortfalls with an inkjet printed foot sole inlay costing $1.85 per sensor, is flexible, runs on nano-watts of power, and can easily be fabricated to personally fit the user's foot. A suite of machine learning algorithms are compared to classify 4 foot movements: sitting, standing, walking, and jogging. Algorithm performance results of the sensor samples show the Support Vector Machine Kernel reaching 83.5% rate of detecting the correct foot movement and classifies 10 times per second. Future work includes embedding the trained algorithm onto a micro-processor, placing it into a shoe sole and performing trials to collect real-world user data such that the technology matures and benefits significantly to those who need a telehealth device for movement monitoring.

Index Terms—inkjet-printed circuits, foot sole sensors, movement monitoring, telehealth devices

I. INTRODUCTION

Cardiovascular disease (CVD) afflicted 18.2% of U.S. citizens aged over 65 years during the year 2020 and remains the number one cause of morbidity in America [1]. Modern telehealth devices for prevention and detection of CVDs are progressing, but still suffer from a critical drawback - the caretakers, family, or home nurses have to manually observe their conditions using simple medical tools like the EKG or stethoscope, with many individuals unaware of their risk until the point of medical intervention [2]. Since the most effective preventative measure shown to lower CVD is 20 minutes of exercise per day, the risk can be mitigated via real-time monitoring of movement activity [3]. While heartbeat monitoring is a useful tool that observes blood flow patterns, detect heart attacks and reduce emergency response time, pressure sensors are an important additional option to characterize the mechanical consequences of patient motion and to track/predict heart failure risks [4]. Pressure sensors have flooded the market as a result, but many of those options are neither easily accessible nor understood by medical staffs, and thus suffer from lack of exposure. Furthermore, pressure sensor designs must meet the critical expectations of comfortable, easy to use, and affordable wearable telehealth devices such as low device weight, cost, environmental impact, and high flexibility, efficiency, reliability and adaptability [5].

The sole of the foot contains critical pressure points that helps quantify patient movement patterns, providing needed data for immediate and long-term health care decisions. Researchers of foot pressure sensors primarily have focused on pressure mapping and manual analysis of electrical signals to help understand implications with respect to their targeted application [6]–[8]. Modern designs often embed bulky electrodes and costly/complex sensors into shoe insoles. This is limiting as every foot applies pressure differently, with multiple types/sizes of shoes often being worn by the same individual, sensitive feet may find the electronics to be uncomfortable and nonviable for regular use.

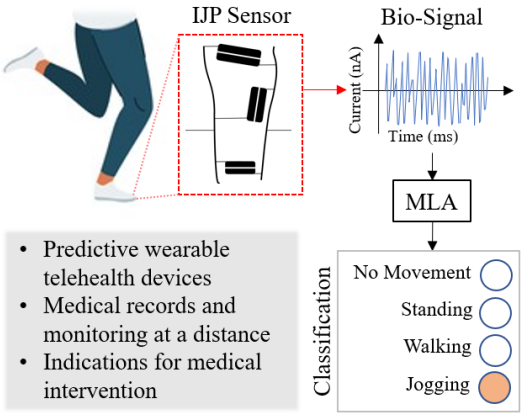

Fig. 1: IJP sensors can be used for cost effective, personal telehealth by monitoring real-time bio-signals and predicting classes to give the signal meaning. The IJP sensor in this work is shown as an example.

As visualized in Fig. 1, a powerful solution to generalization is utilization of machine learning algorithms (MLAs) to identify critical patterns in the sensor signals for predictions [9], [10]. Telehealth devices such as the ones referenced in this work reduce financial burdens of frequent medical check-ups, benefiting the device user, their caretakers, and hospital staff. Detection and prevention at a distance

Corresponding author: M. R. Haider (e-mail: mrhaider@uab.edu).
Digital Object Identifier xx.xxxx/LSENS.xxxx.xxxxxxx

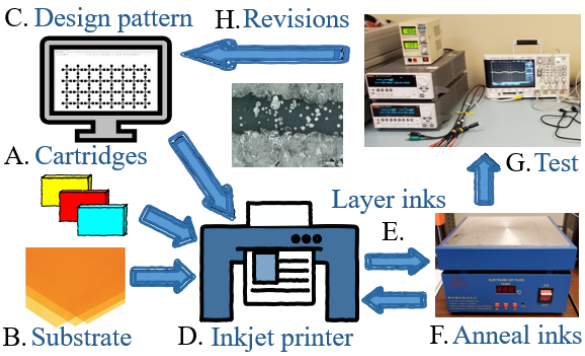

Fig. 2: The IJP circuit fabrication process is shown. A pattern is designed on the computer, printed out layer-by-layer, tested, and revised.

using MLAs is a powerful approach to overcoming inadequacies of modern electronics. Human error is reduced during signal analysis, as features that best identify risk in a given signal may be overlooked or challenging for humans to detect while the computer is impartial to those errors. Adding training data makes the MLAs more robust and generic/task-specific.

This work addresses shortfalls of modern foot sole pressure sensors with the design and testing of a paper-thin inkjet-printed touch-based pressure sensor for movement monitoring. This additive-manufactured sensor is simple, generic, low-cost, low-profile, scalable, physically flexible and smooth to the touch. A suite of MLAs were tested for their ability to identify relative movement based on the electrical signals produced by the sensor. The IJP fabrication process and the sensor's working principle are explained in Sections II and III, respectively, followed by the Foot Sole Pressure Sensor design in Section IV. Data is collected and organized into a dataset for training the MLAs in Section V. The dataset of two samples are used to train 32 MLAs and the best performance is evaluated in Section VI. Lastly, a conclusion to the work is given in Section VII.

II. INKJET-PRINTED TECHNOLOGY

Inkjet printed (IJP) technology takes advantage of piezoelectric printer dynamics to eject uniquely behaving nano-particles from its print head onto a substrate. This growing field of circuit creation has allowed for flexible, biodegradable, repeatable, highly inexpensive, and fast circuit/sensor fabrication, with a plethora of sensing applications that vary according to material choice and circuit structure [11]. The basic IJP process follows the steps as seen in Fig. 2, with several prior works following this scheme [12]–[17]. Nano-particle inks are first filled into refillable cartridges and placed in the inkjet printer. The substrate is then chosen which may be treated prior to printing for improved ink adhesion. Some treated substrates are commercially available, as is chosen for this work (see Section IV). The print patterns are designed on any digital editing program and then the pattern is printed layer-by-layer. Between layers, the substrate may be thermally cured for continuous bulk formation of the nano-particles. The fabrication process varies in research settings to include involved and expensive processes/equipment such as plasma and gas treatment, non-IJP ink deposition, spin-coating, magnetron sputtering, slot-die coding, precise parameter control, usage of novel materials, and many other custom techniques [18].

The silver nanoparticle ink used in this work is non-toxic to humans, in a non-combustible aqueous solution that is eco-friendly, and no sintering is required during fabrication. The nanoparticle diameter is approximately 20 nm and the viscosity is within the range needed to print through home-quality inkjet printer nozzles. The ink cures on the paper within minutes of printing, with no bleeding into the substrate or excess ink coming off from sample interaction.

III. WORKING PRINCIPLE OF THE SENSOR

The equivalent capacitive circuit for two parallel silver plates inkjet printed onto a substrate is shown in Fig. 3. The capacitance formed between these two parallel printed lines can be represented by the famous Palmer's equation. The total capacitance manifests a constant lateral capacitance, C_l, and a fringe capacitance, C_f. The charge, Q, stored across the capacitor due to the constant DC voltage, V, is defined as

$$Q = C \times V = (C_l + C_f) \times V \tag{1}$$

The C_f varies due to the presence of dieletric material of the feet and creates a dynamic current flow to balance the charge equation.

$$i = \frac{dQ}{dt} = V \times \frac{dC_f}{dt} \tag{2}$$

An electromagnetic field (EMF) is generated by the applied voltage in the capacitor model. However, the IJP capacitor's EMF lies beyond the substrate plane, making its capacitance vary based on how the EMF is perturbed by physical interference. The low voltage supply and current output of the IJP sensor causes the EMF of the IJP capacitor to be small, minimizing the unwanted interference.

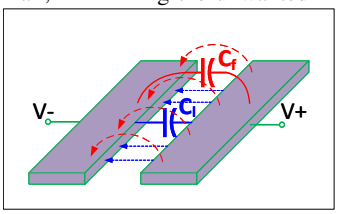

Fig. 3: IJP capacitor working principle. The IJP capacitor emits a small EMF that changes the charge when touched, bent, or deformed.

IV. IJP FOOT SOLE SENSOR FABRICATION

As depicted in Fig. 4, the foot sole sensor is designed as silver (Ag) nanoparticle parallel plates printed onto polyethylene terephthalate (PET) film with a standard drop-on-demand, piezoelectric printer (Epson XP-960). The silver parallel plates are printed with a gap of approximately 0.8 mm, chosen to be above the printer's rated minimum resolution of 0.3 mm to prevent channel shorting via ink splattering. The ink is then annealed by placing the sensor on a hot plate for 5 minutes. The placement of parallel plate nodes were chosen to align with common pressure regions of the foot sole, one at the top bridge, second along the right arch, and third at the heel [19]. Placement of the pressure points is easily customizable according to shoe size and pressure profile. While targeted for elderly movement prediction, the sensor may be adapted for irregular cases such as for amputees, mobile robots, intensive athletics training, etc.

The samples printed for this work are a men's size 9. The substrate thickness is 135 μm and costs \$180 (NB-TP-3GU100 Mitsubishi Paper Mills) for 100 sheets. The cost to print is \$1.85 per sample, estimated from 100 mL bottle of silver nanoparticle ink costing \$120 (NBSIJ-MU01 Mitsubishi Paper Mills) at 220 prints per 11 mL cartridge and \$1.80 per sheet of substrate. The printer and cartridges are one-time costs and not considered in the cost estimation.

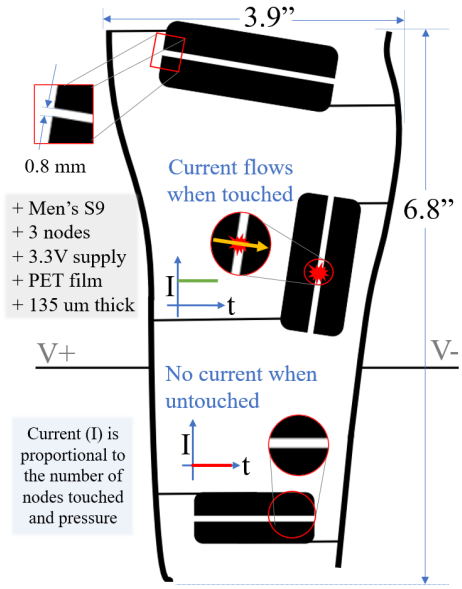

Fig. 4: The Foot Sole Pattern is shown with all relevant dimensions. Without touch, the circuit is open and current is blocked. The current flow through the device increases proportionally to the applied force.

The silver prints used in this work and others have shelf-lives of over 2 years with the most notable degradation being conductivity reduction caused by exposure to standard room-temperature conditions during storage. Visually, the degradation is seen as a change in ink color from silver to yellow-silver. The conductivity degradation over time does change the device biasing but the sensing behavior remains the same. Humidity and temperature are well-known challenges in IJP sensors due to the short-term effects of heightened electron mobility in regions of high humidity/temperature such as in this work, where the sensor will be in a hot and humid shoe during various forms of exercise. Layering temperature- and moisture-resistant inks, polymer covers, and EMI shielding are preventative measures to improve signal reliability before the sensor is ready for patient trials. While the shelf-life of silver-based sensors is long, the sensor will degrade much faster when in use, as the friction and pressure wear the sample down. This primarily affects signal biasing and defines the length of time a single sample may be used. Further studies of sensor lifetime are planned. However, IJP sensors are intended to be quick-use, disposable, and inexpensive options for on-the-go signal collection/analysis.

V. SENSOR DATA COLLECTION

Data is collected for proof-of-concept signal analysis by placing the foot sole sensor onto a flat surface (floor) and covering the sensor with a thin sheet of parchment paper to avoid ink degradation or sensor damage (Fig. 5). The sensor has a positive and negative lead connected to the left and right silver routes extending from the foot sole pattern. Voltage is applied and the current is collected over time with a Keithley 2604B Source Meter. Three trials of data collection for 3 minutes each are performed for each class, for both samples. The full dataset for one sample then contains 36 minutes of data, which is first processed by removing the settle-time data at the start of each signal, and then is divided into window sizes of 0.1 second intervals and labeled by their class so that during run-time the algorithm outputs a prediction 10 times per second. No

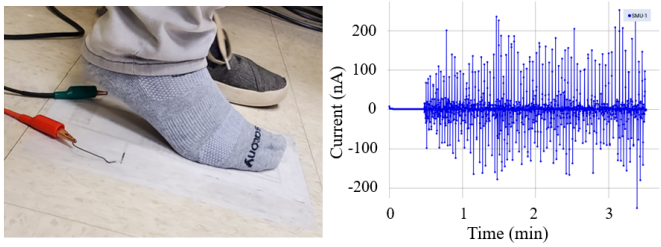

Fig. 5: Example action shot of the data collection process (walking). The IJP Foot Sole Sensor is covered with parchment paper and set in place on the floor prior to data collection.

normalization is performed on the data for design simplicity, and may be added for improved results.

The supply voltage requirement is 3.3 V for compatibility with digital systems. Maximum current flow is 1.4 μA seen in the jogging category, with the maximum power utilization of 4.6 μW. Average power for each class is 14.9 nW (not moving), 13.2 nW (standing), 47.5 nW (walking), and 75.9 nW (jogging). Fig. 6 shows the distribution of combined sample data for each class via box plot. ‘Walking’ and ‘jogging’ show distinct differences to the ‘no movement’ and ‘standing’ classes, seen from the number and magnitude of outliers (red crosses). As a result, the algorithm will have lower accuracy when predicting between ‘no movement’ and ‘standing’. The same box plot metrics were observed for each individual sample and results were consistent with the combined dataset.

VI. RESULTS ANALYSIS

The data of both samples split into 0.1 second intervals and combined into a single dataset makes 2247 total inputs for the MLAs to train/test on. Individually sample 1 has 972 training inputs and sample 2 has 1274. Using MATLAB, 32 MLAs were trained and tested on each sample and the combined dataset according to the four movement classes, with the top performing algorithms shown in Fig. 7 and the best MLA shown as a confusion matrix in Fig. 8. The worst performing algorithms across all samples were eliminated from consideration as the ideal MLA for foot sole movement monitoring. The more powerful algorithms such as the neural network and kernels are capable of finding more complex features within the dataset.

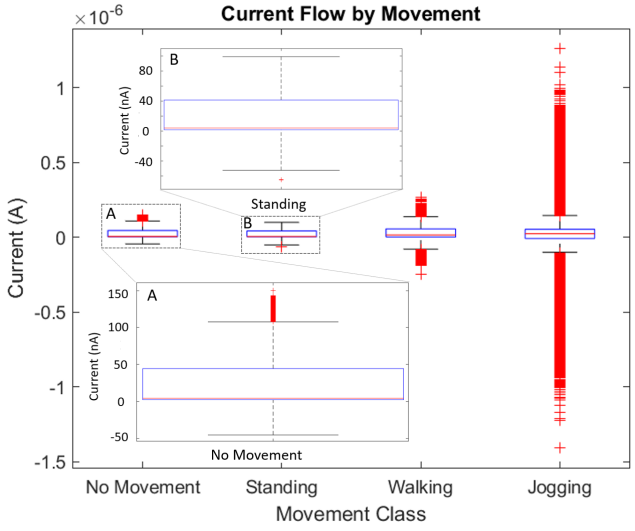

Fig. 6: The concatenated data (current flow) from the samples are shown as box plots for each movement class.

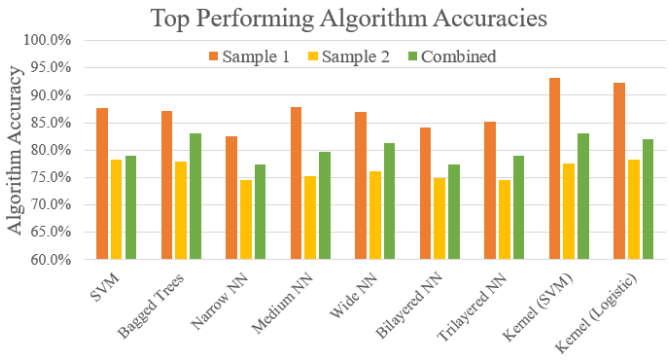

Fig. 7: The best performing MLAs are shown for the samples and combined dataset.

Kernels allow for higher dimensions of training and therefore better accuracy. For instance, the SVM performs at 79% in the combined dataset but the highest accuracy MLA of this work (SVM Kernel) reaches 83.5% simply due to deeper analysis of the signal features. Similarly, logistic regression is heavily used for binary predictions but within the Kernel is applied to more dimensions for multiple class outcomes, making its performance competitive at 82% accuracy. Sample 1 had higher prediction accuracy across all MLAs and is attributed to the more distinct distribution of collected data for each class. Sample 2 had significantly lower accuracy across all MLAs trained, making the combination of both samples an indicator that poor selectivity in a given trial run benefits from the greater performances of other trial runs.

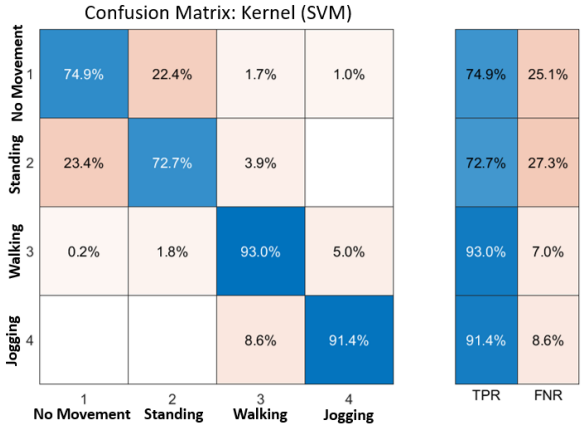

Fig. 8: The kernel (SVM) confusion matrix shows the combined dataset prediction versus the true outputs.

VII. CONCLUSION

Inkjet printing of a low-cost, smooth, and flexible foot sole sensor was performed in this work by designing a simple foot pattern and printing it onto PET film with silver nanoparticle ink. Current flow data was collected over time by placing the sensor onto a sturdy surface and performing the movement action ('no movement', 'standing', 'walking', and 'jogging'). No movement and standing have less distinction, thus are classified at lower accuracies and will benefit from training on greater sample sizes. The top performing MLA for the samples is the SVM Kernel at 83.5% prediction accuracy as it can apply the SVM at higher dimensions, finding the features needed to predict the correct movement class. The IJP sensor approach presented here is a step towards an adaptable solution for low-profile movement monitoring.

VIII. ACKNOWLEDGMENT

This research was supported by USA National Science Foundation (ECCS-2201447 and ECCS-1813949), and U. S. Army Research Center Phase V – Cooperative Agreement (1.A83, W56HZV-19-2-0001). Any opinions, findings, conclusions, or recommendations expressed herein are those of the authors and do not necessarily reflect the funding agency's views. A special thanks to Mr. Ryan Edwards for helping gathering the data, and Dr. J. Iwan D. Alexander and Dr. Sazia Eliza for their valuable reviews.

REFERENCES

[1] "Quickstats: Percentage of adults aged over 18 years with diagnosed heart disease, by urbanization level and age group - national health interview survey, united states," *Morb Mortal Weekly Report (MMWR)*, vol. 71, no. 778, 2022.

[2] C. L. Snoswell, M. L. Taylor, T. A. Comans, A. C. Smith, L. C. Gray, and L. J. Caffery, "Determining if telehealth can reduce health system costs: Scoping review," *J Med Internet Res*, vol. 22, no. 10, p. e17298, 2020.

[3] C. Barbiellini Amidei, C. Trevisan, M. Dotto, E. Ferroni, M. Noale, S. Maggi, M. C. Corti, G. Baggio, U. Fedeli, and G. Sergi, "Association of physical activity trajectories with major cardiovascular diseases in elderly people," *Heart*, vol. 108, no. 5, pp. 360–366, 2022.

[4] S. Mishra, S. Mohanty, and A. Ramadoss, "Functionality of flexible pressure sensors in cardiovascular health monitoring: A review," *ACS Sensors*, vol. 7, no. 9, pp. 2495–2520, 2022.

[5] C. Ferguson, L. D. Hickman, S. Turkmani, P. Breen, G. Gargiulo, and S. C. Inglis, "'wearables only work on patients that wear them': Barriers and facilitators to the adoption of wearable cardiac monitoring technologies," *Cardiovasc Digit Health J*, vol. 2, no. 2, pp. 137–147, 2021.

[6] V. Bucinskas, A. Dzedzickis, J. Rozene, J. Subaciute-Zemaitiene, I. Satkauskas, V. Uvarovas, R. Bobina, and I. Morkvenaite-Vilkonciene, "Wearable feet pressure sensor for human gait and falling diagnosis," *Sensors (Basel)*, vol. 21, no. 15, 2021.

[7] B. Jasiewicz, E. Klimiec, M. Młotek, P. Guzdek, S. Duda, J. Adamczyk, T. Potaczek, J. Piekarski, and G. Kołaszczyński, "Quantitative analysis of foot plantar pressure during walking," *Med Sci Monit*, vol. 25, pp. 4916–4922, 2019.

[8] M. Fuchs, M. Hermans, H. Kars, J. Hendriks, and M. van der Steen.

[9] C. Kuziemsky, A. J. Maeder, O. John, S. B. Gogia, A. Basu, S. Meher, and M. Ito, "Role of artificial intelligence within the telehealth domain," *Yearb Med Inform*, vol. 28, no. 1, pp. 35–40, 2019.

[10] O. C. Oguine and K. J. Oguine, "Ai in telemedicine: An appraisal on deep learning-based approaches to virtual diagnostic solutions (vds)," 2022. [Online]. Available: https://arxiv.org/abs/2208.04690

[11] M. A. Shah, D.-G. Lee, B.-Y. Lee, and S. Hur, "Classifications and applications of inkjet printing technology: A review," *IEEE Access*, vol. 9, pp. 140 079–140 102, 2021.

[12] R. Lu, M. R. Haider, S. Gardner, J. I. D. Alexander, and Y. Massoud, "A paper-based inkjet-printed graphene sensor for breathing-flow monitoring," *IEEE Sensors Letters*, vol. 3, no. 2, pp. 1–4, 2019.

[13] M. T. Islam, S. D. Gardner, R. Lu, M. R. Haider, J. I. D. Alexander, and Y. Massoud, "A low-cost planar inkjet-printed carbon nanotube field effect transistor for sensor applications," in *2019 IEEE 62nd International Midwest Symposium on Circuits and Systems (MWSCAS)*, 2019, pp. 734–737.

[14] S. D. Gardner, M. T. Islam, J. I. D. Alexander, Y. Massoud, and M. R. Haider, "A carbon nanotube inkjet-printed hybrid circuit for non-conventional computing," in *2020 IEEE 63rd International Midwest Symposium on Circuits and Systems (MWSCAS)*, 2020, pp. 373–376.

[15] S. D. Gardner, M. R. Haider, M. T. Islam, J. I. D. Alexander, and Y. Massoud, "Aluminum-doped zinc oxide (zno) inkjet-printed piezoelectric array for pressure gradient mapping," in *2019 IEEE 62nd International Midwest Symposium on Circuits and Systems (MWSCAS)*, 2019, pp. 1101–1104.

[16] S. D. Gardner, J. I. D. Alexander, Y. Massoud, and M. R. Haider, "An inkjet-printed paper-based flexible sensor for pressure mapping applications," in *2020 IEEE International Symposium on Circuits and Systems (ISCAS)*, 2020, pp. 1–5.

[17] ——, "Minimally produced inkjet-printed tactile sensor model for improved data reliability," in *2020 11th International Conference on Electrical and Computer Engineering (ICECE)*, 2020, pp. 49–52.

[18] H. Matsui, Y. Takeda, and S. Tokito, "Flexible and printed organic transistors: From materials to integrated circuits," *Organic Electronics*, vol. 75, 2019.

[19] M. Grdzelidze, "A statistical evaluation and analysis of the results of shoes wear test method for a pilot study," *Magyar Tudomanyos Journal*, pp. 30–34, 11 2017.